Multiple rows of cells behind an epithelial wound edge extend cryptic lamellipodia to collectively drive cell-sheet movement

Rizwan Farooqui and Gabriel Fenteany*

Department of Chemistry, University of Illinois at Chicago, 845 West Taylor Street, Chicago, IL 60607, USA

*Author for correspondence (e-mail: fenteany@uic.edu)

Accepted 4 October 2004
Journal of Cell Science 118, 51-63 Published by The Company of Biologists 2005
doi:10.1242/jcs.01577

Summary

The mechanism by which epithelial, endothelial and other strongly cell-cell adhesive cells migrate collectively as continuous sheets is not clear, even though this process is crucial for embryonic development and tissue repair in virtually all multicellular animals. Wound closure in Madin-Darby canine kidney (MDCK) epithelial cell monolayers involves Rac GTPase-dependent migration of cells both at and behind the wound edge. We report here for the first time that cells behind the margin of wounded MDCK cell monolayers, even hundreds of microns from the edge, extend 'cryptic' lamellipodia against the substratum beneath cells in front of them, toward the wound, as determined by confocal, two-photon and transmission electron microscopy. These so-called submarginal cells nevertheless strictly maintain their more apical cell-cell contacts when they migrate as part of a coherent cell sheet, hiding their basal protrusions from conventional microscopy. The submarginal protrusions display the hallmarks of traditional lamellipodia based on morphology and dynamics. Cells behind the margin therefore actively crawl, instead of just moving passively when cells at the margin pull on them. The rate of migration is inversely proportional to the distance from the margin, and cells move co-ordinately, yet still in part autonomously, toward the wound area. We also clarify the ancillary role played by nonprotrusive contractile actin bundles that assemble in a Rho GTPase-dependent manner at the margin after wounding. In addition, some cell proliferation occurs at a delay after wounding but does not contribute to closure. Instead, it apparently serves to replace damaged cells so that intact spread cells can revert to their normal cuboidal morphology and the original cell density of the unbroken sheet can be restored.

Supplementary material available online at
http://jcs.biologists.org/cgi/content/full/118/1/51/DC1

Key words: Collective cell migration, Epithelial cell sheet, Wound closure, Lamellipodia, Membrane protrusion

Introduction

The migration of cells as continuous sheets is much less studied but no less important a phenomenon than the migration of cells as single free entities. Cell-sheet migration is a form of collective cell motility, especially characteristic of epithelial cells both in vivo and in vitro, which obey the maxim that 'an epithelium will not tolerate a free edge' (Rand, 1915; Trinkaus, 1984). Disruption of an epithelium through scratching, scraping or cutting initiates the process of wound closure, driven by the migration of the cells into the wound area. Epithelial cells generally maintain their various cell-cell contacts when they migrate as a coherent sheet to close the gap. Wound closure in cultured epithelial cells resembles cell-sheet movement in vivo during the re-epithelialization process in wound healing and during embryonic morphogenesis, such as in dorsal closure in *Drosophila melanogaster* (for reviews, see Harden, 2002; Jacinto et al., 2002; Martin and Parkhurst, 2004), ventral enclosure in *Caenorhabditis elegans* (for a review, see Simske and Hardin, 2001) and eyelid closure in mouse (for a review, see Martin and Parkhurst, 2004).

How do epithelial cell sheets generate force to migrate as a collective? In bilayered *Xenopus laevis* epidermal cell sheets, basal cells appear to spread underneath one another during cell-sheet migration (Radice, 1980a; Radice, 1980b; Strohmeier and Bereiter-Hahn, 1991). However, in contrast to other epithelial cell systems that strictly maintain cell-cell contacts during sheet migration without any discontinuity in the monolayer observed at any time, small gaps appear to briefly open up between cells in the migrating *Xenopus* epidermis (Radice, 1980b). This allows so-called submarginal cells behind the leading edge of the advancing sheet to extend protrusions into the area temporarily vacated by the retracting trailing edges of cells in front of them, with the stimulus for submarginal protrusion possibly being the transient availability of an unoccupied substratum for spreading of submarginal cells. Newt epidermal cell sheets appear to migrate in a similar fashion (Donaldson and Dunlap, 1981; Mahan and Donaldson, 1986). Furthermore, in the mouse corneal epithelium, which is composed of two to three cell layers behind the margin of an introduced wound, submarginal cells have – in cross section – a tapered profile that may reflect lamellipodial protrusion

Journal of Cell Science

(Danjo and Gipson, 1998; Danjo and Gipson, 2002). Whereas a mechanism, in which individual cells near the wound margin repeatedly crawl or 'leapfrog' over one another, has been proposed for wound healing in stratified epithelia and is supported by some experimental evidence (Danjo and Gipson, 2002; Garlick and Taichman, 1994; Gibbins, 1978; Krawczyk, 1971; Quilhac and Sire, 1999), there is also evidence that stratified epithelial wounds instead close by migration as a coherent sheet in a sliding fashion that resembles cell-sheet movement in monolayer cultures (Buck, 1979; Hanna, 1966; Radice, 1980b; Zhao et al., 2003).

Certain nonepithelial cells can also migrate as continuous sheets, such as wounded endothelial cell monolayers (for a review, see Lee and Gotlieb, 2003) and *Xenopus* mesendodermal cells (Davidson et al., 2002). During invasion and metastasis of epithelial and vascular tumors that are not fully de-differentiated, as well other cancers like melanomas and rhabdomyosarcomas, cells can migrate in groups as sheets, strands or clusters (for reviews, see Friedl, 2004; Friedl et al., 2004; Friedl and Wolf, 2003). Similar collective cell movements occur during epithelial and endothelial tube morphogenesis, including development of the neural tube, lung, kidney, mammary and digestive glands, urogenital tract and vasculature (for reviews, see Lubarsky and Krasnow, 2003; Nelson, 2003). A range of other tissue movements and sheet dynamics are also central to embryogenesis (for reviews, see Colas and Schoenwolf, 2001; Keller, 2002; Keller et al., 2003; Trinkaus, 1984).

Cell migration involves regulated actin filament assembly and membrane protrusion, and also cell-substratum adhesion for traction, actin disassembly behind the leading edge, cell body translocation, detachment from the substratum and trailing-edge retraction (for reviews, see Carlier et al., 2003; Fenteany and Zhu, 2003; Pollard and Borisy, 2003; Rafelski and Theriot, 2004; Revenu et al., 2004; Ridley et al., 2003; Small et al., 2002; Welch and Mullins, 2002). Actin dynamics are controlled by a large number of proteins, from effectors of signal transduction to actin-binding proteins that modulate the state of the actin cytoskeleton. Members of the Rho family of Ras-related small GTPases, in particular, play central roles in the control of actin dynamics, cell migration and other cellular processes (for reviews, see Burridge and Wennerberg, 2004; Raftopoulou and Hall, 2004). Activation of Rho isoforms – the prototype members of this family – leads to the formation of contractile actomyosin bundles, such as stress fibers, and the assembly of focal adhesions. Rac isoforms are involved in membrane ruffling and lamellipodial protrusion. Cdc42 is implicated in filopodial extension and the control of cell polarity. Although these functions are distinct, there is signaling crosstalk among the different Rho-family small GTPases.

Because of their reliably epithelial character, Madin-Darby canine kidney (MDCK) epithelial cells are one of the most extensively used cell lines in epithelial cell biology and a major model system for studying numerous epithelial functions. MDCK cells can move in two distinct modes: as dispersing individual cells following treatment of subconfluent two-dimensional cultures with hepatocyte growth factor/scatter factor or as continuous sheets that strictly maintain cell-cell contacts following mechanical disruption of confluent monolayers. Closure of wounds in MDCK cell monolayers involves Rac-, phosphoinositide- and c-Jun-N-terminal-kinase-dependent cell migration (Altan and Fenteany, 2004; Fenteany et al., 2000). Motile force generation during wound closure in MDCK cell sheets appears to take place in multiple rows of cells from the wound margin in the continuous migrating cell sheet, allowing the cells to move in a collective fashion (Fenteany et al., 2000). Microinjection of dominant-negative Rac1 into the first row of cells prevents lamellipodial protrusion at the margin yet does not hinder wound closure, whereas microinjection into all the cells in the first three rows blocks closure. In addition, Rac-dependent actin polymerization in multiple rows of cells is observed after wounding. Cells behind the margin of moving epithelial cell sheets, usually referred to as submarginal cells (Trinkaus, 1984), therefore appear not to be simply passive and pulled forward by crawling marginal (wound-edge) cells, as has been suggested (Dipasquale, 1975; Kolega, 1981; Vaughan and Trinkaus, 1966); instead, they can also generate Rac-dependent locomotory force by themselves (Fenteany et al., 2000). Because submarginal cells in the migrating cell sheet strictly maintain their more apical cell-cell contacts on all sides, any basal protrusive activity in these submarginal cells would be obscured under other cells with imaging by conventional microscopic methods that do not provide good *z*-axis information.

After wounding MDCK cell monolayers, thick apical bundles of filamentous actin (F-actin) form at the wound edge in a Rho-dependent manner, although they are not continuous around the margin (Fenteany et al., 2000). Rho activity and marginal actin bundles are not required for wound closure to occur within a normal time frame in MDCK cell monolayers, in contrast to actomyosin contraction-based purse-string systems (for reviews, see Bement, 2002; Jacinto et al., 2001; Kiehart, 1999; Martin and Parkhurst, 2004; Redd et al., 2004; Woolley and Martin, 2000). Instead, marginal actin bundles in wounded MDCK cell monolayers contribute to making the edge advance more evenly, so that wound closure is more uniform and regular (Fenteany et al., 2000), possibly by stabilizing the margin and helping to distribute force from more actively protruding marginal cells to neighboring marginal cells. Furthermore, like Rho, Cdc42 is not required for wound closure in MDCK cell monolayers and little filopodial protrusion is visible, although Cdc42 is also involved in helping to determine the regularity of wound closure, possibly through its effect on cell polarity.

In this study, we establish that submarginal cells of the wounded MDCK cell sheet extend 'cryptic' lamellipodia basally under cells in front of them and crawl actively against the substratum while maintaining cell-cell contacts. We characterize the protrusive activity and migratory behavior of submarginal cells as a function of distance from the wound edge, and clarify the roles of marginal actin bundles and cell proliferation in restoration of the cell monolayer.

Materials and Methods

Reagents

Minimum Essential Medium (with Earle's balanced salts, nonessential amino acids, L-glutamine, sodium pyruvate and 2.1 g/l sodium bicarbonate) and lipofectamine were purchased from Gibco/Invitrogen. Newborn calf serum was from Biowhittaker. 5-Bromo-

2′-deoxyuridine (BrdU), Alexa Fluor 488-conjugated anti-BrdU antibody and Alexa Fluor 488-conjugated anti-IgG secondary antibody were from Molecular Probes. Tetramethylrhodamine isothiocyanate-conjugated phalloidin (TRITC-phalloidin) was from Sigma-Aldrich. H-1152, Y-27632, ML-7, (±)-blebbistatin, mitomycin C (MMC) and Mowiol 4-88 were from Calbiochem. The enhanced green fluorescent protein (GFP)-human β-actin fusion under the control of a 3-kb fragment of the human β-actin promoter cloned into pcDNA3 is described elsewhere (Ballestrem et al., 1998).

Cell culture and stable transfection

MDCK epithelial cells were purchased from the American Type Culture Collection. Cells were maintained in growth medium consisting of minimum essential medium with 10% newborn calf serum and grown at 37°C with 5% CO_2 in a humidified tissue culture incubator. Cells were not used beyond 12 passages and were from frozen stock cultures (stored in liquid N_2). MDCK cell lines expressing GFP-actin were generated by transfection of the GFP-actin construct into MDCK cells using lipofectamine (Gibco/Invitrogen), according to the manufacturer's protocol. Selection and maintenance of stable transfectants were carried out with 500 μg/ml G418 sulfate (Geneticin®, Gibco/Invitrogen) in growth medium. Following limiting dilution, individual colonies were transferred with cloning disks for expansion on new tissue culture plates and then evaluated for homogeneous expression levels. From among the highest GFP-actin-expressing clones, a single cell line was selected for experimental use.

Wound closure and cell tracking

MDCK cells were plated in 24-well tissue culture plates at an initial density of 2×10^5 cells/well. Inhibitors from stock solutions in dimethyl sulfoxide (DMSO) or double-distilled water (ddH_2O) were added to confluent cultures with fresh growth medium 30 minutes before wounding, unless indicated otherwise. Control cultures were treated with the corresponding final concentration of carrier solvent alone. Circular scratch wounds of ~500 μm in diameter were made using a micropipet with 10-μl pipet tip, and cells were kept at 37°C and 5% CO_2 during the experiment. Wound closure was followed by phase-contrast microscopy on a Zeiss Axiovert 25 microscope, and digital images of the entire wound area were acquired as a function of time following wounding using a Roper Scientific CoolSNAP-Pro charge-coupled device (CCD) camera and RS Image software. Concurrent with image acquisition, the number of lamellipodia around the wound edge was counted for subsequent determination of lamellipodial density at the margin (number of lamellipodia divided by wound margin perimeter length). Images were analyzed using the public domain ImageJ program (developed at the National Institutes of Health and available on the Internet at http://rsb.info.nih.gov/ij/) on an Apple Power Macintosh computer. Progress of wound closure was quantitated from digital images by tracing the margin perimeter and determining remaining open wound area as a function of time, as previously described (McHenry et al., 2002). Following each experiment, cell viability was confirmed by the Trypan Blue dye exclusion assay.

For cell-tracking experiments, cells were plated on Bioptechs culture dishes at 3×10^5/dish and grown to confluence, at which time rectangular wounds (~700 μm in width by ~18 mm in length) were made by scratching with a flame-blunted microinjection needle attached to a Narishige micromanipulator. Images of the cell sheet migrating in a Bioptechs Delta TC3 culture dish system at 37°C were acquired every 10 minutes over 12 hours after wounding by automated time-lapse microscopy using an Zeiss Axiovert 200 microscope with Uniblitz shutter (Vincent Associates), a Zeiss AxioCam HR CCD camera and Openlab software (Improvision). Cell centroid (center of mass) positions were later determined using Openlab software for individual cells in the sheet at different distances perpendicular to the wound margin over time. In addition, we tracked pairs of cells within a given cell row initially located immediately next to or at a centroid-centroid distance of ~200-300 μm from one another to evaluate relative movements of nearest neighbors compared to more distant pairs of cells within a row. Individual cell centroid paths were plotted, and rates of cell migration determined.

Fluorescence analysis of cell-sheet migration

For visualization of submarginal protrusions by confocal microscopy, MDCK cells expressing GFP-actin were mixed with nontransfected cells at a ratio of 1:10 and plated on glass coverslips in 12-well tissue culture plates at 3×10^5 cells/well in growth medium. Upon reaching confluence, cell monolayers were wounded (with an initial wound size of ~700 μm in width by ~18 mm in length). Cells were kept at 37°C and 5% CO_2 during wound closure and then fixed 6 hours later with 3.7% formaldehyde, permeabilized with 0.1% Triton X-100 and stained with TRITC-phalloidin, all in phosphate-buffered saline (PBS), as previously described (Fenteany et al., 2000). Coverslips were mounted on slides in Mowiol 4-88 (0.1 g/ml) mounting medium and then imaged using a Zeiss LSM 510 laser scanning confocal microscope on an Axiovert 100M, equipped with 40× C-Apochromat (1.2 NA, water) and 63× C-Apochromat (1.2 NA, water) objectives and photomultiplier tube detector. The 488- and 568-nm lines of the argon/krypton laser were used to excite GFP and TRITC, respectively. Images were acquired using Zeiss LSM software in the multitrack mode for clear separation of GFP and TRITC signals.

For quantitation of the parameters of submarginal protrusion, wounding and fixation was performed as described above, and acquired images were analyzed using OpenLab software. For quantitation of marginal protrusion, the wounded cell monolayers were examined by phase-contrast microscopy, instead of fluorescence, which allowed for clear visualization of the border between cell body and protrusion for marginal cells. Digital images were again analyzed using OpenLab software.

Dynamic activity of submarginal protrusions was visualized by two-photon microscopy as follows. MDCK cells (1:10 ratio of GFP-expressing:nontransfected cells) were plated on Bioptechs culture dishes at 3×10^5 cells/dish and grown to confluence. Rectangular wounds (~700 μm in width by ~18 mm in length) were then generated using a flame-blunted microinjection needle. Images of the cell sheet migrating in a Bioptechs Delta TC3 culture dish system at 37°C were captured every 10 minutes from immediately after wounding to 4 hours post-wounding. A custom-built two-photon laser scanning microscope on a Zeiss Axiovert 200M platform was used for imaging, as described previously (Stahelin et al., 2004), with a Spectra Physics Tsunami tunable ultrafast laser set for femtosecond pulses at 920 nm, a 100× Plan-Apochromat (1.4 NA, oil) objective and a customized Peltier-cooled Hamamatsu R1477-style photomultiplier tube detector. The microscope was controlled and images acquired using the SimFCS program written by Enrico Gratton (University of Illinois, Urbana-Champaign, IL).

In experiments involving conventional fluorescence microscopy, samples were examined on a Zeiss Axiovert 200 microscope with 40× Plan-Neofluar (0.75 NA, air) or 63× Plan-Neofluar (1.25 NA, oil) objectives. Images were acquired with a Zeiss AxioCam HR CCD camera and Openlab software.

Transmission electron microscopy

MDCK cells were plated on 60-mm diameter tissue culture dishes at 1.5×10^6 cells/dish and grown to confluence. The cell monolayers were then wounded with a flame-blunted microinjection needle, and cells were incubated at 37°C and 5% CO_2 during wound closure. Twelve hours after wounding, the cells were rinsed 3 times with PBS and fixed with 3% glutaraldehyde in 0.1 M cacodylate buffer (pH 7.4) at room temperature. The fixed monolayers were contrasted with 1%

osmium tetraoxide for 1 hour and dehydrated with increasing concentrations of ethanol. Samples were then embedded in Epon 812 resin, and thin sections perpendicular to the wound margin were made using a Leica Ultracut UCT ultramicrotome. Slices were further contrasted with 2% uranyl acetate and 2% lead citrate and mounted on 200 mesh copper grids. Images were acquired using a JEOL JEM 1220 electron microscope and Gatan Digital Micrograph 2.5.8 software.

Cell proliferation experiments

MDCK cells were plated on glass coverslips in 12-well tissue culture plates at 3×10^5 cells/well in growth medium. Confluent monolayers were incubated in the presence or absence of MMC, added with fresh growth medium. After 48 hours, medium was again changed to fresh growth medium with or without MMC. Narrow, rectangular wounds (~200 μm in width by ~18 mm in length) were made that closed by 12 hours, and cells were kept at 37°C and 5% CO_2 during this time. In other experiments, wider wounds were made that closed by 24-36 hours. Unwounded monolayers were used to assess the level of contact-inhibited cell proliferation in parallel. Subconfluent cultures were also prepared to determine the proliferation rate of noncontact-inhibited MDCK cells as a reference. At different times after wounding, cells were incubated with 10 μM BrdU for 2 hours. Cells were then fixed in 1:1 methanol:acetone at 20°C. Coverslips were placed in 4 N HCl, followed by incubation in 3% BSA/0.2% Triton X-100 in PBS and then with Alexa Fluor 488-conjugated anti-BrdU antibody in 80% blocking buffer/20% PBS. To visualize all nuclei, DNA was stained with 1 μg/ml propidium iodide in 2× saline-sodium citrate buffer/0.2% Triton X-100. Coverslips were mounted on slides in Mowiol 4-88 mounting medium and examined by conventional fluorescence microscopy. All nuclei in each field of view were used for analysis. Percentage of BrdU-positive cells was determined from the ratio of BrdU-positive nuclei over total propidium iodide-stained nuclei.

Results

Submarginal cells extend cryptic lamellipodia with leading-edge characteristics

While cells at the margin of wounded MDCK cell monolayers obviously extend lamellipodia, protrusive activity in cells behind the margin is not visible by phase-contrast microscopy (see supplementary material, Movie 1) and not clearly identifiable by differential interference contrast microscopy, even with optical sectioning. We therefore sought other means to discover whether submarginal cells extend any hidden lamellipodia. Comparison of cell morphologies and wound-closure rates between GFP-actin-expressing and nontransfected MDCK cells revealed no detectable difference (data not shown). We therefore mixed GFP-actin-expressing MDCK cells with nontransfected MDCK cells in a 1:10 ratio and then analyzed the cell monolayers by confocal microscopy after wounding. We found that lamellipodia clearly protrude from submarginal cells in the direction of movement toward the wound (Fig. 1A,B). Orthogonal profiles at the bottom (*xz*) and to the left (*yz*) of the central *xy* images show that green GFP-actin signal extends basally against the substratum underneath nontransfected cells, which are red owing to staining of actin filaments with TRITC-phalloidin. This is especially clear in the *xz* orthogonal profile at the bottom of Fig. 1A. In addition, protruding nontransfected cells that are wedged under GFP-actin-expressing cells in front of them show a purely red basal signal. By ~15 cell rows (which equals ~300 μm, based on an average cell diameter of 20 μm) from the wound margin, cells resemble those in unwounded monolayers and are more densely packed; whereas less spread than cells closer to the margin, they display a small amount of wedging under neighboring cells (Fig. 1C, Table 1).

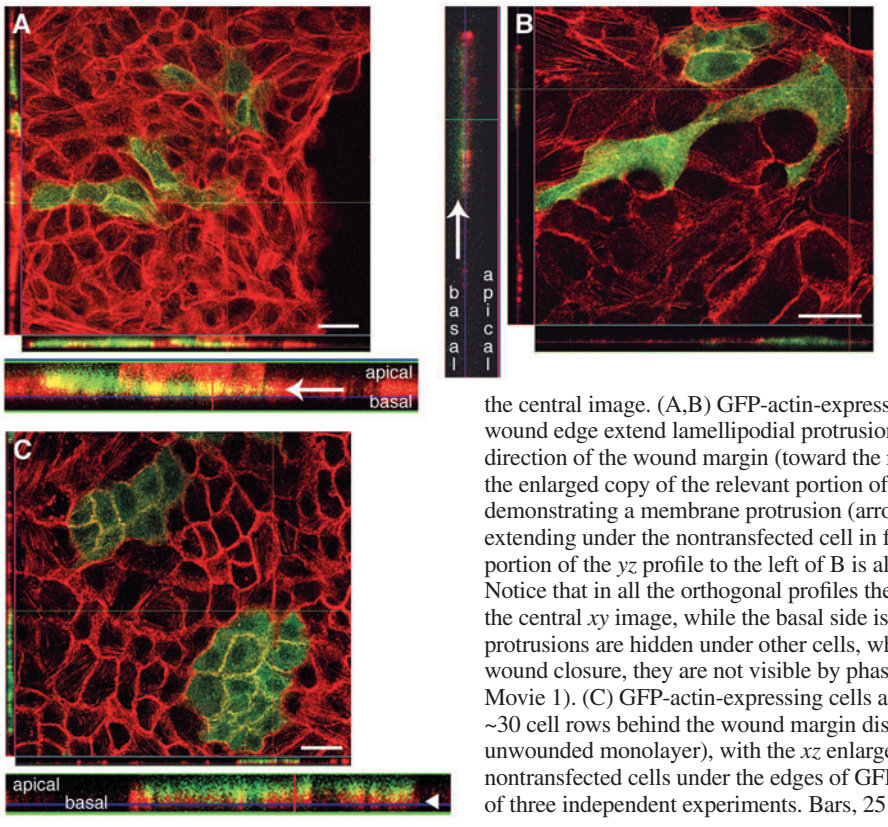

Fig. 1. Submarginal cells in a migrating epithelial cell sheet extend cryptic lamellipodia in the direction of the wound margin. MDCK cell monolayers composed of GFP-actin expressing cells (green) grown with nontransfected cells in a 1:10 ratio were fixed 6 hours after wounding, permeabilized, stained for F-actin with TRITC-phalloidin (red) and imaged by confocal microscopy. The initial width of the rectangular wounds was ~700 μm. In all images, the orthogonal *z*-stack profiles (0.20-0.25-μm slices) along the indicated lines in the *x* or *y* dimension of the central *xy* image are shown in the rectangular windows at the bottom (*xz*) and to the left (*yz*) of the central image. (A,B) GFP-actin-expressing and nontransfected cells located behind the wound edge extend lamellipodial protrusions basally underneath cells in front of them in the direction of the wound margin (toward the right side in both images). This is especially clear in the enlarged copy of the relevant portion of the *xz* orthogonal profile at the bottom of A, demonstrating a membrane protrusion (arrow) from a GFP-actin-expressing cell (green) extending under the nontransfected cell in front of it (red). An enlarged copy of the relevant portion of the *yz* profile to the left of B is also shown, again with a basal protrusion (arrow). Notice that in all the orthogonal profiles the apical side of the monolayer is directly adjacent to the central *xy* image, while the basal side is on the outside. Because the submarginal protrusions are hidden under other cells, which remain in contact with one another throughout wound closure, they are not visible by phase-contrast microscopy (see supplementary material, Movie 1). (C) GFP-actin-expressing cells and nontransfected cells pictured between ~20 and ~30 cell rows behind the wound margin display just a small amount of spreading (similar to the unwounded monolayer), with the *xz* enlargement showing some wedging (arrowhead) of nontransfected cells under the edges of GFP-actin-expressing cells. Images are representative of three independent experiments. Bars, 25 μm.

Transmission electron microscopy also reveals basal protrusive structures emanating from submarginal cells and extending under the trailing edges of cells more proximal to the wound margin (Fig. 2A-D). These cells are highly spread and squamous in appearance, distinct from the more cuboidal morphology of cells in the unwounded portion of the monolayer, although even in the unwounded monolayer some spreading of cells underneath each other is observed (Fig. 2E), consistent with the orthogonal section in Fig. 1C and the quantitative data in Table 1. Furthermore, various cell-cell contacts are clearly present and apical to the looser areas around the membrane protrusions.

Table 1. Quantitative parameters of membrane protrusion in the migrating epithelial cell sheet

Distance[†]	Cells protruding[‡] (%)	Protruding cells facing margin[§] (%)	Protrusion length (μm)[¶]	Protrusion area (μm^2)**
Margin	34.1±1.7*	100	16.6±0.9*	549±48*
0-100 μm	51.3±6.9*	70.8±7.2	10.4±1.9*	160±37*
100-200 μm	38.8±6.7*	82.5±6.4	10.9±1.4*	104±9*
200-300 μm	26.7±5.8	74.2±7.0	7.2±0.9	99±14
Unwounded	13.5±1.2	N/A (randomly oriented)	6.0±0.4	67±8

MDCK cell monolayers (1:10 ratio of GFP-actin expressing cells and nontransfected cells) were fixed, permeabilized and stained for F-actin with TRITC-phalloidin 6 hours after wounding. The initial width of the wounds was ~700 μm.

*P<0.05 by unpaired Student's t test compared to the unwounded monolayer.

[†]Distance from the margin was measured along a straight line from and perpendicular to the wound margin to each GFP-actin-expressing cell.

[‡]Percentage of GFP-actin-expressing cells with measurable membrane protrusions in any direction was determined using those cells in a cluster of GFP-actin-expressing cells for which protrusions could be discerned projecting under neighboring cells divided by the total number of GFP-actin-expressing cells in each random field of view. Values are weighted average± s.e.m. for n=23 random fields of view for the margin (and a total of 211 cells); n=29 random fields of views each for the three different submarginal zones (and a total of 160 cells each for 0-100 μm and 100-200 μm, and 120 cells for 200-300 μm); n=20 random fields of view for the unwounded monolayer (229 cells). Each data set was derived from at least three independent experiments. Two caveats must be kept in mind. First, because any protrusions extending under other GFP-actin-expressing cells are not detectable, the numbers may be undercounts of the actual proportion of protruding cells. Second, although we have observed no difference in morphology or wound closure rate with GFP-actin-expressing cells compared to nontransfected cells, it is possible that the degree of submarginal protrusiveness may differ between the two.

[§]Percent of submarginal protrusions oriented toward the wound margin (within±60° of the axis perpendicular to the margin) was determined from the set of protruding cells. Values are weighted average±s.e.m. for the relevant subset of cells in the preceding column). Each data set was derived from at least three independent experiments. In the unwounded monolayer, cell spreading is randomly oriented.

[¶]Protrusion length at the margin was measured from the farthest point of the lamellipodial tip to the cell body, using phase-contrast micrographs for marginal cells, which allow for clear visualization of the border between cell body and protrusion. Submarginal protrusion length was measured from the farthest point of a basal protrusion extending from a GFP-actin-expressing cell to the TRITC-phalloidin-stained F-actin associated with the adhesion belt of the cell under which the protrusion projects (approximately the point of apical cell-cell contact), using fluorescence micrographs. Mean±s.e.m. is shown for: n=49 cells at the margin; n=9 cells from 0-100 μm behind the margin; n=11 cells from 100-200 μm; n=6 cells from 200-300 μm; n=31 cells from the unwounded monolayer). Each data set was derived from at least three independent experiments. Sample sizes were limited by the number of cells in random fields of view for which precise protrusion lengths and areas could be unambiguously determined.

**Protrusion area was determined concurrently with the length measurements in the preceding column for the same cells (mean±s.e.m.). Protrusions at the margin tend to be longer and broader than submarginal ones.

Submarginal protrusions are also discernible in xy images (Figs 1, 3, 5). They form shortly after wounding and exhibit lamellipodial morphology and dynamics in basal xy images by two-photon microscopy (Fig. 3; see also supplementary material, Movie 2). As expected, neither submarginal nor marginal protrusions form in wounded monolayers treated with the actin-disrupting agents cytochalasin D or latrunculin B, and wound closure is completely inhibited by these inhibitors of actin polymerization (data not shown).

A significant proportion of marginal and submarginal cells extend membrane protrusions (Table 1). The maximal percentage of cells protruding is not observed at the wound margin but rather in the first 100 μm behind it, with a progressive decrease in frequency the further away the cells are from the wound edge. The bulk of the submarginal protrusions in wounded monolayers are oriented toward the margin. Although there is clearly significant protrusive activity above baseline to at least 200 μm behind the margin, individual membrane protrusions are, on average, longer and broader at the margin, and the length and area of protrusions decline with distance from the edge. There is also some spreading of cells in the unwounded monolayer; however, this is randomly oriented and does not exhibit a directional bias.

Submarginal cells migrate coordinately yet partly autonomously

Cell-tracking experiments show that the rate of migration of individual cells in the advancing sheet is inversely related to distance from the margin (Fig. 4). Marginal and submarginal cells move toward the wound with overall persistence, although not all moving submarginal cells are migrating in the direction of the wound at any given time and cells can change directions and migrate in an oblique manner (Fig. 4; see also supplementary material, Movie 1). Movements of individual cells during wound closure are correlated with those of neighboring cells at all distances from the margin, yet each cell's movement is still somewhat independent of the other. While two neighboring cells in a cell row will tend to move in parallel toward the wound margin, there are short-range changes in direction that are not in tandem but appear more independent. The apparent coordination of cell movements decreases with increasing distance between two cells in a given cell row.

Wound closure is independent of marginal actin bundle formation and contraction

To probe the roles of the Rho- and myosin-light-chain-kinase pathways, and formation and contraction of marginal actomyosin bundle in wound closure, MDCK cell monolayers were treated with the Rho-kinase inhibitors H-1152 (Ikenoya et al., 2002) and Y-27632 (Uehata et al., 1997), the myosin light chain kinase inhibitor ML-7 (Saitoh et al., 1987) or the nonmuscle and skeletal-muscle-myosin-II inhibitor (±)-blebbistatin, of which (–)-blebbistatin is the active enantiomer (Straight et al., 2003). All of these inhibitors decrease formation of the marginal actin bundles that normally assemble apically and discontinuously around the margin after wounding, and also reduce stress fiber numbers (Fig. 5 and data

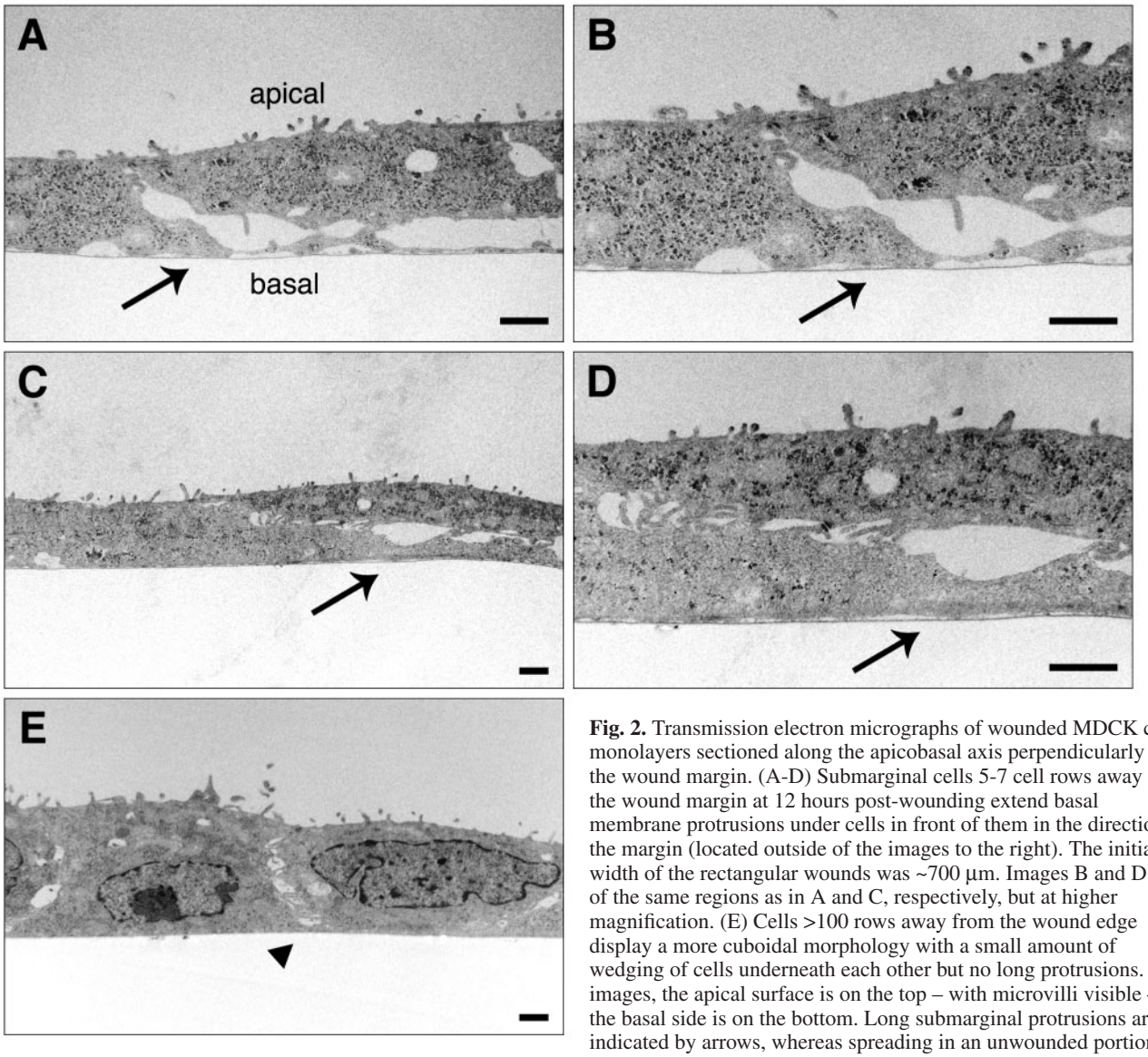

Fig. 2. Transmission electron micrographs of wounded MDCK cell monolayers sectioned along the apicobasal axis perpendicularly to the wound margin. (A-D) Submarginal cells 5-7 cell rows away from the wound margin at 12 hours post-wounding extend basal membrane protrusions under cells in front of them in the direction of the margin (located outside of the images to the right). The initial width of the rectangular wounds was ~700 μm. Images B and D are of the same regions as in A and C, respectively, but at higher magnification. (E) Cells >100 rows away from the wound edge display a more cuboidal morphology with a small amount of wedging of cells underneath each other but no long protrusions. In all images, the apical surface is on the top – with microvilli visible – and the basal side is on the bottom. Long submarginal protrusions are indicated by arrows, whereas spreading in an unwounded portion of monolayer is indicated by an arrowhead. Notice the different close cell-cell contacts apical to the looser areas around the basal protrusions, allowing sheet continuity to be maintained simultaneously with the extension of lamellipodia. All of the MDCK cells in this and subsequent figures are nontransfected, unless otherwise noted. Bars, 1 μm.

not shown). In the closure progress curves, a very slight acceleration of wound closure appears after treating cells with H1152 or blebbistatin but is not statistically significant by Student's *t* test (Fig. 6A,B and data not shown). There are also slight increases in protrusive activity at the margin (Fig. 6C,D and data not shown). Submarginal protrusion may also be more extensive following treatment with these inhibitors, as particularly apparent in Fig. 5B, and protrusion in general appears morphologically aberrant, especially after treatment with blebbistatin (Fig. 5C). In addition, treatment results in slightly less regular wound closure (Fig. 6E,F).

Delayed cell proliferation is triggered by wounding but is not involved in wound closure

To assess any possible contribution of cell proliferation to re-epithelialization in MDCK cell monolayers, we incubated the cells with BrdU for a 2-hours period – starting at different time points in the wound healing process – and analyzed for BrdU incorporation into the newly synthesized DNA of any cells that were in S phase. After the generation of narrow wounds of ~200 μm across, a transient burst in the proliferation rate is apparent by 12 hours, (Fig. 7A,B). By this time, these narrow wounds have completely closed and the cells covering the former wound area are in their most spread state, as evident in Fig. 7A. For wider wounds that close by 24-36 hours, the peak in BrdU-positive cells is ~24 hours after wounding (data not shown). However, treatment with MMC, which completely blocks MDCK cell proliferation (data not shown), has no significant effect on the rate of wound closure in MDCK cell monolayers (Fig. 7C).

Discussion

Wound closure in cultured epithelial cells provides a tractable

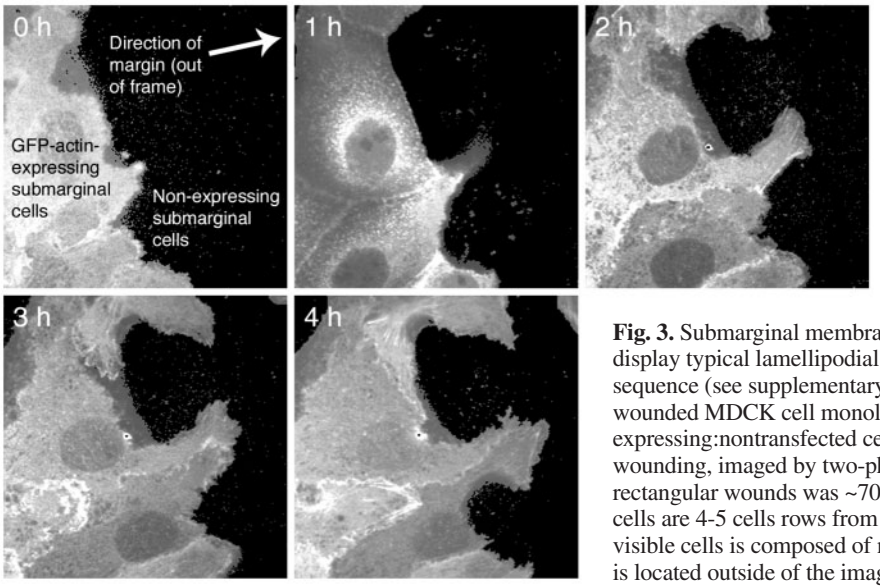

Fig. 3. Submarginal membrane protrusions form shortly after wounding and display typical lamellipodial morphology and dynamics. Panels from a time-lapse sequence (see supplementary material, Movie 2) of a basal focal plane of a wounded MDCK cell monolayer (1:10 ratio of GFP-actin-expressing:nontransfected cells) immediately after wounding to 4 hours post-wounding, imaged by two-photon microscopy. The initial width of the rectangular wounds was ~700 μm. The visible GFP-actin-expressing submarginal cells are 4-5 cells rows from the wound margin. The dark area to the right of the visible cells is composed of nontransfected submarginal cells. The wound margin is located outside of the images to the right in the direction of the arrow.

model system for studying the process of cell-sheet migration. Most previous studies have focused on the easily observable dynamics at the wound edge. By contrast, protrusive activity in the cells behind the margin has remained obscure. Suggestively, even in phase-contrast time-lapse sequences of the migrating MDCK cell sheet, not all submarginal cells appear to move constantly toward the wound margin in an orderly fashion (see supplementary material, Movie 1). Instead, although the cells move toward the wound area, some submarginal cells move at oblique angles to the margin at any given time, supporting the notion that they individually generate force and are not just being pulled by cells in front of them. We show here that cells distal to the wound edge respond to wounding by extending lamellipodia with typical leading-edge characteristics against the substratum underneath cells in front of them toward the wound margin (Figs 1-3, Table 1; supplementary material, Movie 2). In fact, compared to marginal cells, a higher proportion of submarginal cells in the first ~100 μm from the wound edge protrude, possibly because marginal actin bundles locally antagonize membrane protrusion, although the lamellipodia tend to be longer and broader at the margin (Table 1). Together with previous results (Fenteany et al., 2000), our new data strongly suggest that submarginal cells in the moving cell sheet actively generate their own motile force by a protrusive crawling mechanism, rather than just remaining passive and being pulled by locomoting marginal cells.

TRITC-phalloidin-stained F-actin is prominent in stress fibers and around the perimeter of all the cells in the MDCK cell sheet (Fig. 1, Fig. 5A). The circumferential actin bundles around the perimeter of the cells are primarily associated with the cadherin-based adherens junctions (adhesion belts) and to a lesser extent the tight junctions, and are apical to the visible basal protrusions that project from the GFP-actin-expressing cells. Adherens junctions, along with intermediate filament-linked desmosomes, are the major mechanically relevant cell-cell adhesion complexes in epithelia, responsible for preserving the continuity of the cell sheet. Tight junctions are the most apical of the junctional complexes. Although they are also actin filament-linked, tight junctions do not have such a significant mechanical function but rather serve as a transepithelial permeability barrier and are important for apicobasal polarization, demarcating the apical and basolateral plasma membrane domains. Because cell-cell contacts are maintained throughout the whole process of wound closure, submarginal lamellipodia protrude under other cells and, therefore, could be called cryptic.

The signals that first initiate MDCK cell protrusion and migration in marginal cells in response to wounding, and the mechanism by which submarginal cells 'sense' the presence of the wound and also begin migrating directionally are not known. Soluble factors, either passively released from damaged cells or actively secreted by intact cells, may be involved, as may factors associated with extracellular matrix deposited by cells. Exogenously supplied epidermal growth factor and low concentrations of hepatocyte growth factor/scatter factor are each capable of accelerating wound closure in MDCK cell monolayers (Sponsel et al., 1994), as are certain nucleotides discussed further below (Kartha and Toback, 1992; Sponsel et al., 1995). However, it has not been determined whether MDCK cells normally actively produce autocrine factors that stimulate closure after wounding, which appears the case for transforming growth factor-β (TGF-β) in bronchial epithelial wound repair (Howat et al., 2002). In MDCK cell monolayers, exogenously supplied TGF-β1 impairs wound closure (Sponsel et al., 1994). We have hitherto seen little or no effect of either the potent and selective epidermal growth factor receptor tyrosine kinase inhibitor PD 153035 (AG 1517) or a function-blocking anti-pan-TGF-β antibody on wound closure (data not shown). Another possible mechanism involves temporary plasma membrane damage to the still viable cells directly abutting the new free edge, which become more permeable to extracellular factors for a time after wounding. For example, upon wounding of cultured corneal epithelial cells, there is an immediate influx of Ca^{2+} from the medium in marginal cells only, which may be owing to such an effect, distinct from subsequent waves of Ca^{2+} released from intracellular stores in submarginal cells (Klepeis et al., 2001). Endogenous electric fields, coupled with Ca^{2+} and growth

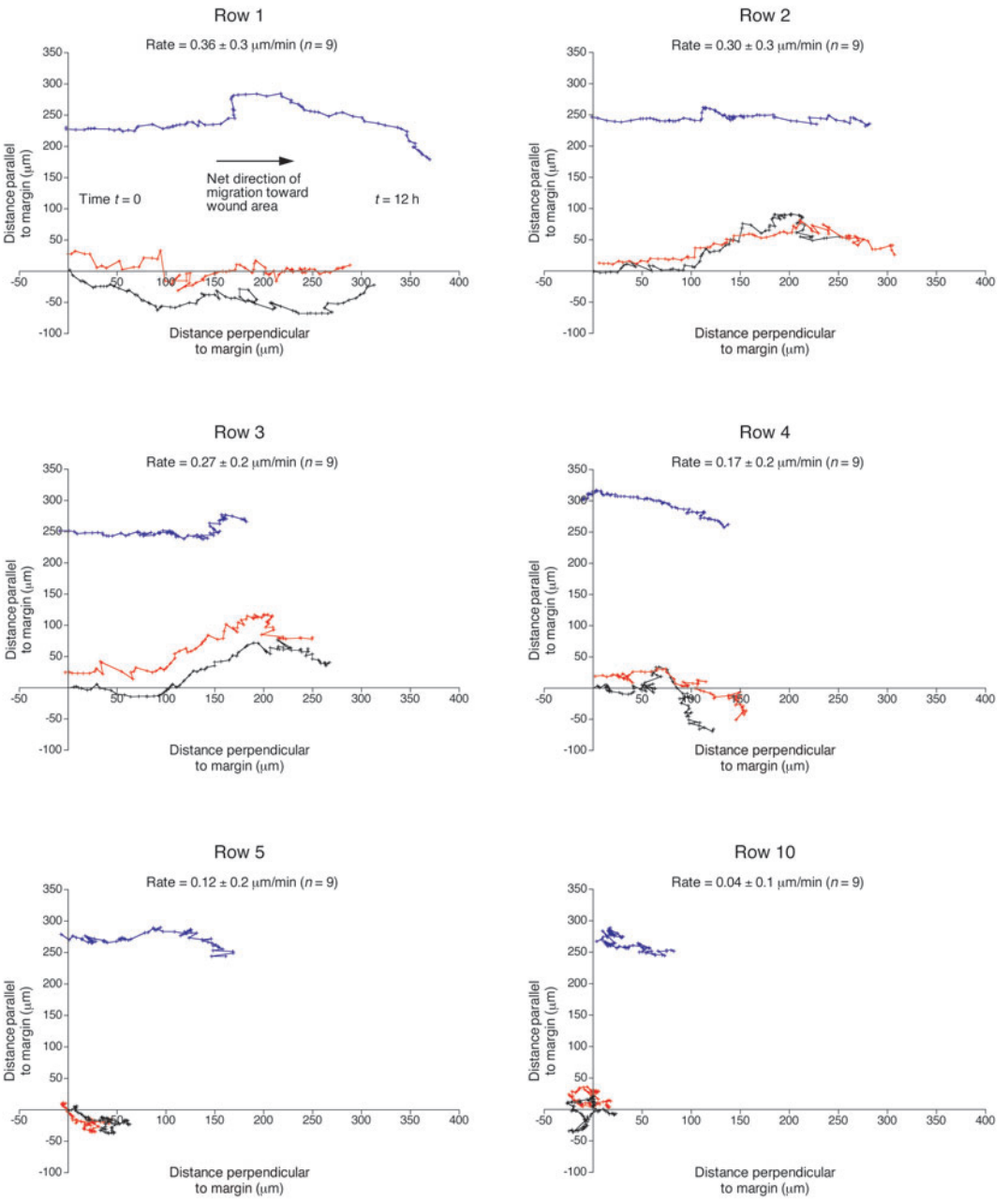

Fig. 4. The rate of cell migration is inversely proportional to the distance from the wound edge, and cells move along related, though still partly independent, paths toward the wound area. The row number refers to rough distance from the wound margin in terms of cell rows, with row 1 being cells at the margin, and rows 2-5 and 10 being submarginal cells progressively further from the edge of the cell sheet. Centroids from individual cells in the wounded MDCK cell monolayer were tracked for 12 hours after wounding. The initial width of the rectangular wounds was ~700 μm. Each graph represents the paths of three cells, all in the same cell row at a similar distance from the margin: a reference cell (black), a directly neighboring cell (red) and another more distant cell (blue). Marks in each trace represent the centroid positions of a single cell at 10-minute intervals. Cell paths were tracked along *x* and *y* coordinates (the axes perpendicular and parallel to the wound margin, respectively). Traces are representative of three independent experiments. The statistical rates of displacement along the *x* axis toward the wound area over the period of 0 to 12 hours for each row of cells are indicated at the top of each graph. Rates are mean ± s.e.m. in μm/minute calculated from traces shown and others not shown for a total of *n*=9 cells for each row position from three separate wounds.

factor signaling, may also be involved in triggering the wound healing response (for a review, see Nuccitelli, 2003).

Finally, there is the possibility that creation of a free edge can trigger migration simply by the removal of physical constraints, allowing cells already primed for motility to move into a new area cleared of the 'barriers' posed by other cells, a hypothesis for which there is some support in corneal epithelial cell sheets (Block et al., 2004). Cells in the intact epithelium could therefore be viewed as constantly sampling their mechanical environment by pushing and pulling on neighboring cells in a random manner without polarization or directional persistence. There is a small degree of randomly oriented spreading of cells underneath one another even very far from the wound margin and in unwounded monolayers (Fig. 1C and Fig. 2E, Table 1). Furthermore, in time-lapse sequences of unwounded monolayers, MDCK cells can be seen to very slowly change positions relative to one another without ever breaking the continuity of the cell sheet (data not shown). Cell-cell contacts and sheet continuity, while strictly maintained, are dynamic. Mature E-cadherin-based adherens junctions and desmosomes, as well as tight junctions and gap junctions, must be disassembled and new ones established simultaneously as cells swap positions. The slow shifting of relative cell positions is evidence that some form of active movement of individual cells within the sheet is an intrinsic property of the epithelium, because the cells are too large and

adhesive for this to be a diffusional process. Further evidence for this being an active process is that the spreading and slow movement and position-switching depend on actin polymerization even in the unwounded monolayer, as inhibitors of actin polymerization freeze out these movements (data not shown).

The cells may thus be primed for a rapid protrusive and migratory response should a gap open up. Changes in the mechanical environment associated with wounding could then lead to activation of signaling pathways, like the Rac pathway, above basal levels for more active spreading and migration. Polarization and directional migration into the wound area could therefore result from hyper-activation of the epithelium's intrinsic dynamics, occurring by default through a stimulated though mechanically biased 'random walk' when spatial constraints in one direction are eliminated upon wounding. This becomes more plausible when one considers the accumulating evidence that changes in the distribution of mechanical forces in and around cells can modulate intracellular signaling pathways and trigger specific biochemical and cellular responses (for reviews, see Bershadsky et al., 2003; Goldmann, 2002; Ingber, 2003; Janmey and Weitz, 2004).

In addition to the question of how protrusion and migration are initiated in the first row, there is also the related yet distinct problem of how the signal to polarize and migrate is then propagated from marginal to submarginal cells? How are cells distal to the wound edge stimulated to crawl toward the wound even though they are not directly abutting the gap? Soluble signals emanating from the margin and transmitted from cell to cell through gap junctions or through extracellular intermediates may serve in directional sensing and movement. Propagation of the signal could potentially involve intracellular Ca^{2+} waves moving back from marginal to submarginal cells. Interestingly, it is known that cell-to-cell gap-junction-independent cytosolic Ca^{2+} waves are initiated by wounding in corneal epithelial cells, and extracellular ATP or UTP appear to mediate propagation of these waves (Klepeis et al., 2001). Similar results were obtained following wounding of alveolar epithelial cells (Hinman et al., 1997; Isakson et al., 2001). Furthermore, in MDCK cell monolayers, exogenously supplied ADP, ATP and UTP can accelerate wound closure (Kartha and Toback, 1992; Sponsel et al., 1995).

We have so far observed little or no effect on wound closure in MDCK cell monolayers from different intracellular Ca^{2+}-modulating treatments, including BAPTA-AM (the cell-permeant and intracellular esterase-cleaved acetoxymethyl ester derivative of the Ca^{2+} chelator BAPTA to deplete intracellular but not extracellular Ca^{2+}), thapsigargin (an inhibitor of the endoplasmic reticulum Ca^{2+}-ATPase) or the Ca^{2+} ionophore A23187 (data not shown). Similar negative results were obtained following treatment of MDCK cells with apyrase, which hydrolyzes ATP and ADP in the extracellular milieu, and the purinergic receptor inhibitors suramin or 5′-*p*-fluorosulfonylbenzoyladenosine (data not shown). In addition, submarginal protrusion does not appear to require communication through gap junctions in MDCK cells, as the gap junction blockers 18-β-glycyrrhetinic acid and dieldrin do not inhibit extension of lamellipodia following wounding (data not shown). Replacement of the medium every 15 minutes after wounding also does not inhibit protrusion (data not shown),

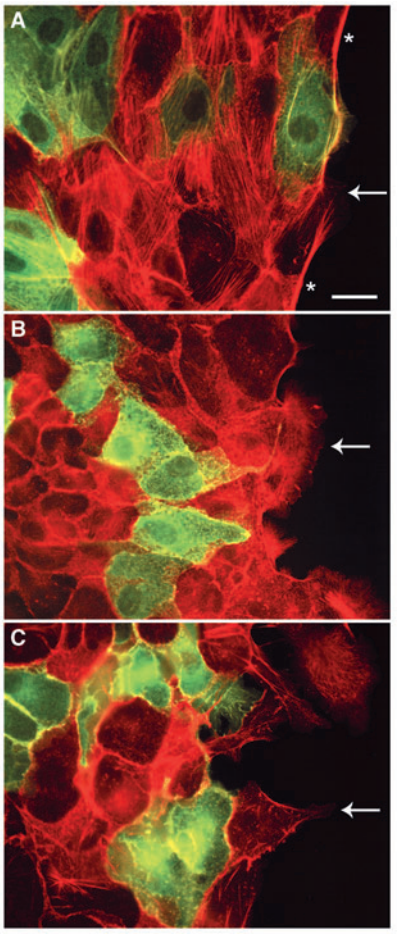

Fig. 5. Inhibition of Rho-kinase or nonmuscle myosin II results in decreased marginal actin bundle and stress fiber numbers and staining intensity. MDCK cell monolayers (1:10 ratio of GFP-actin expressing cells and nontransfected cells) were fixed, permeabilized and stained for F-actin with TRITC-phalloidin 6 hours after wounding following treatment with (A) 0.2% DMSO carrier solvent, (B) 50 μM H1152, a Rho-kinase inhibitor, or (C) 100 μM (±)-blebbistatin, a nonmuscle and skeletal muscle myosin II inhibitor. The initial width of the rectangular wounds was ~700 μm. Similar results were obtained with Y-27632, another Rho-kinase inhibitor, and ML-7, a myosin light chain kinase inhibitor. Marginal actin bundles are indicated by asterisks, whereas membrane protrusions are indicated by arrows. Submarginal protrusions are also discernable in these images. Images are representative of at least three independent experiments in each case. Bar, 25 μm.

although it is possible that rapidly acting diffusible secreted factors may still be involved in the initiation or propagation of motility. Finally, protrusion in either marginal or submarginal cells does not require de novo gene expression because treatment with the protein synthesis inhibitor cycloheximide does not significantly affect formation of lamellipodia at 1-3 hours after wounding, although continued protrusion at later times is affected, presumably as general protein levels run down (Altan and Fenteany, 2004) (data not shown).

A simple and attractive alternative is that directional movement of submarginal cells instead arises from biochemical and mechanical stimulation through cytoskeleton-linked cell-cell adhesion complexes, such as adherens

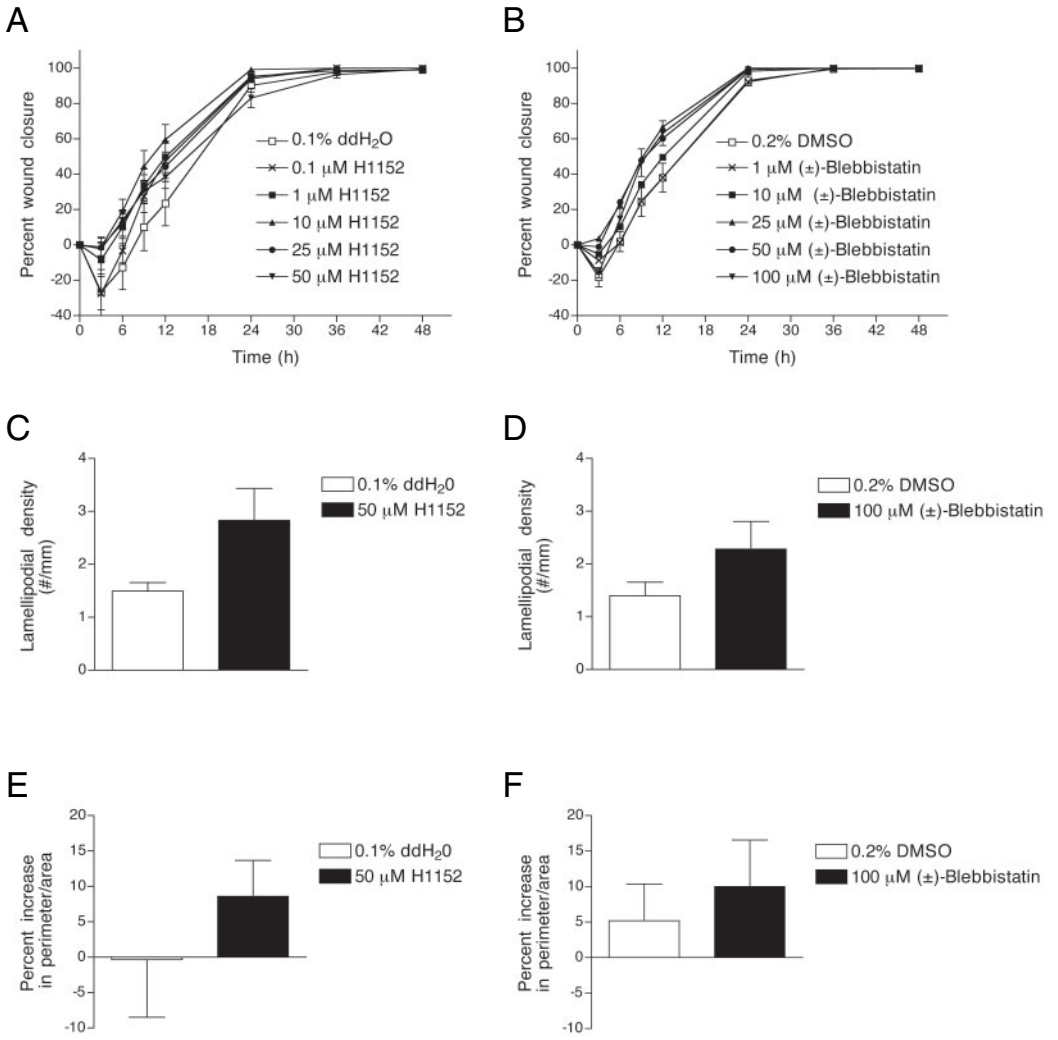

Fig. 6. Inhibition of Rho-kinase or nonmuscle myosin II slightly increases protrusive activity and slightly decreases the regularity of wound closure. Progress of wound closure in MDCK cell monolayers in the presence or absence of H1152 (A) or (±)-blebbistatin (B). The initial diameter of the circular wounds was ~500 μm. Lamellipodial density at 6 hours after wounding (number of lamellipodia at the wound margin and dividing by margin perimeter length) in the presence or absence of H1152 (C) or (±)-blebbistatin (D). Regularity of wound closure (percent increase from 0 to 6 hours after wounding in the quotient of margin perimeter length divided by area) in the presence or absence of H1152 (E) or (±)-blebbistatin (F). Data are mean and s.e.m. for n=12 individual wounds in separate wells on multiwell tissue culture plates from three independent experiments for each treatment at each indicated concentration.

junctions and desmosomes. Submarginal cells may be triggered to polarize in direct response to the movement of the cells at the margin, which may tug on the cells behind them, serving as a stimulus for polarization and migration in the same direction. This could be part of a direction-sensing mechanotransduction mechanism or simply the default consequence of the displacement of the barrier formed by the marginal cells as they sweep forward, making the same direction mechanically less resistant to movement of cells behind the margin. In addition, it is known that actin filaments align parallel to an axis of applied stress in epidermal cells, and this prevents protrusion in any direction that is not parallel to the tension (Kolega, 1986). Therefore, given that the cells all remain connected, pulling from the retracting trailing edges of margin-proximal cells on more distal cells could cause filament alignment in the distal cells, further biasing protrusion and migration of submarginal cells in the same direction as marginal cells.

The rate of migration is inversely proportional to a cell's distance from the wound margin, and the paths of neighboring cells as they migrate toward the wound area are roughly parallel at all distances from the margin (Fig. 4). However, cells still exhibit signs of migratory autonomy with uncoupled short-range directional changes. Even with nearby cells, one may be moving straight toward to the margin while the other moves at a more oblique angle at any given time (Fig. 4; see also supplementary material, Movie 1). Nearby cells, therefore, move coordinately but not in absolute lockstep, and this coordination decreases with increasing distance between cells. These results further support the argument that individual submarginal cells generate their own force for movement, while maintaining biochemical and mechanical relationships

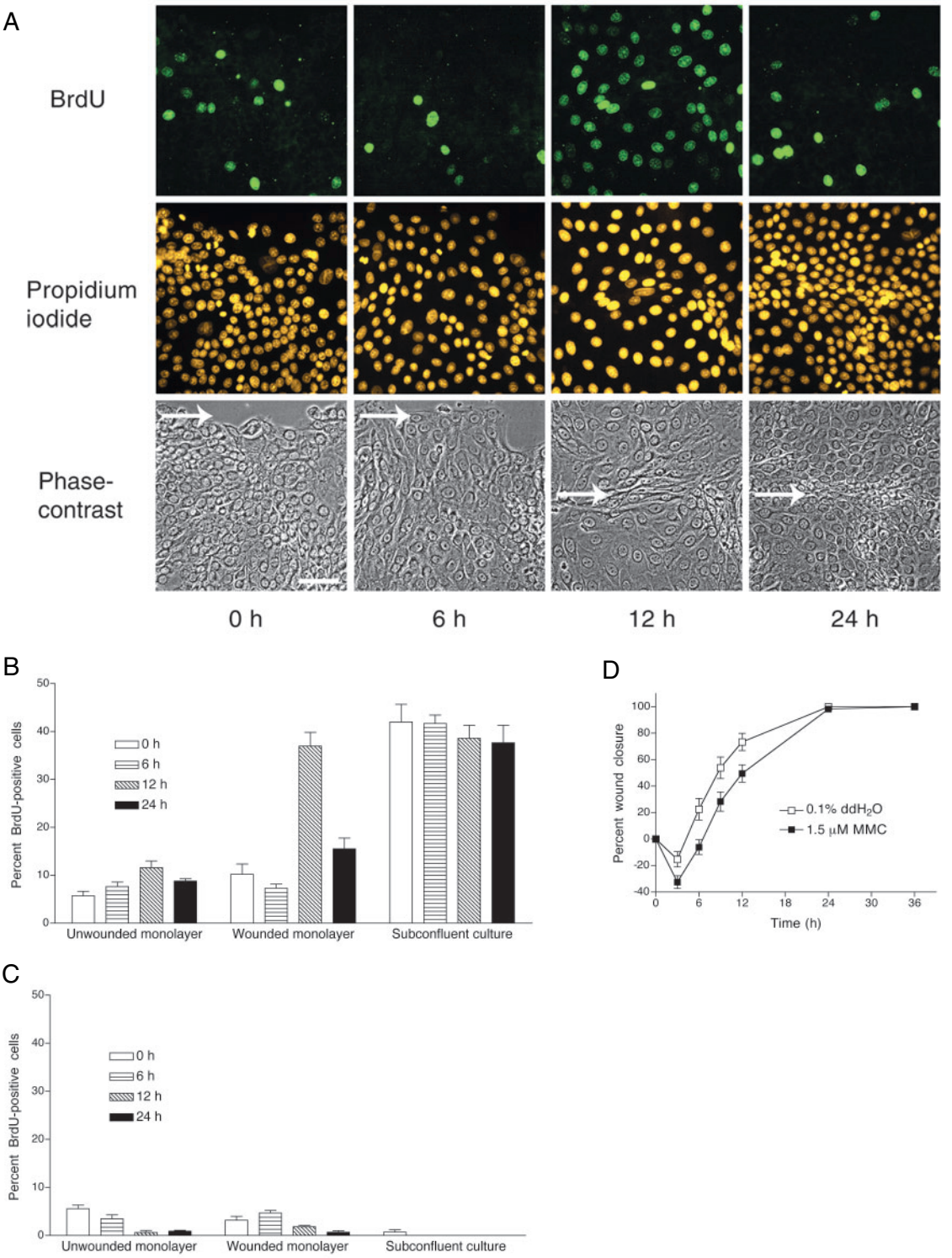

Fig. 7. Wounding triggers delayed cell proliferation but inhibition of proliferation does not affect wound closure. (A) Fluorescence and corresponding phase-contrast images showing BrdU incorporation over the course of wound closure in fixed MDCK cell monolayers. The initial width of the rectangular wounds in A-C was ~200 μm. Arrows indicate location of wound margin at 0 and 6 hours, edge-edge contact at 12 hours or former wound area at 24 hours. Bar, 50 μm. In other experiments, wider wounds were made that closed by 24-36 hours, and similar results were obtained, with BrdU incorporation peaking ~24 hours (data not shown). (B) Percentage of BrdU-positive nuclei for wounded monolayers as a function of time after wounding, as well as parallel unwounded monolayers and subconfluent cultures (mean and s.e.m.; n=15 fields of view from three independent experiments). (C) The DNA-alkylating agent mitomycin C (MMC, 1.5 μM) blocks MDCK cell proliferation based on BrdU incorporation as in B, as well as the tetrazolium salt assay, with no evidence of general toxicity as assessed by Trypan Blue dye exclusion (data not shown). (D) Wound closure in the presence and absence of MMC added 48 hours before wounding (mean and s.e.m. for n=24 wounds). The initial diameter of the circular wounds in this experiment was ~500 μm.

with their neighbors. Partly independent cell motility and sheet continuity are simultaneously possible because spreading occurs basally against the substratum, while the different cell-cell contacts are apical to any membrane protrusions (Fig. 2). In a sense, cell-sheet migration could be viewed as simply the product of a large number of individual cells crawling toward a region of low mechanical resistance, but cells happen to be tethered to one another and so appear to generally move together. Of course, the actual degree of communication and coordination certainly far exceeds that implied by such a minimalist notion, but this could still be the essence of the process.

Myosin II isoforms bundle and contract actin filaments. Perturbation of the formation, stability and function of such actomyosin bundles results in decreased marginal actin bundle and stress fiber staining (Fig. 5). Although not required for closure, marginal actin bundles may function to distribute force from more protrusive cells to their neighbors in the first row, thereby making the wound margin more even and regular as it sweeps forward. Intense marginal F-actin staining in nonprotrusive cells to either side of a highly protrusive cell is often observed, and the smooth arced contour of the edge in these nonprotrusive cells suggests a margin under tension (Fenteany et al., 2000) (Fig. 5A; see also supplementary material, Movie 1). Cells that are protruding at any given time display less marginal F-actin staining, and formation and contraction of marginal actomyosin bundles and stress fibers in MDCK cells may be antagonistic to membrane protrusion and spreading (Figs 5, 6). It has also been shown that inhibition of the Rho pathway results in greater protrusive activity at the margin of wounded rat liver epithelial monolayers (Omelchenko et al., 2003) and slightly accelerated wound closure in bronchial epithelial cells (Desai et al., 2004).

Whereas we observed a delayed transient increase in cell proliferation after wounding, narrower wounds are completely closed by the time the S-phase peak is observed, and complete pharmacological blockage of proliferation does not affect the rate of wound closure (Fig. 7). In addition, serum is not required for wound closure in MDCK cell monolayers, which occurs at the same rate after serum deprivation as with serum (Altan and Fenteany, 2004). These findings are in agreement with a previous report showing that inhibition of MDCK cell proliferation by irradiation with ultraviolet light does not affect wound closure (Sponsel et al., 1994) and are consistent with previous observations (Fenteany et al., 2000). Because some cells are irrevocably damaged and die even with careful mechanical wounding and generation of small wounds, the role of proliferation is probably to restore the initial cell density and morphology, controlled homeostatically by an unknown mechanism in epithelia. MDCK cell monolayers have a strong tendency to maintain a relatively constant cell density, which influences both proliferation and migration (Rosen and Misfeldt, 1980). When cells spread and migrate to close the wound, each comes to cover a greater area of the substratum than originally. Cell proliferation allows final restoration of the higher cell density characteristic of the unbroken monolayer. The spread cells can thus revert to their original cuboidal morphology, at which point their growth and division are contact-inhibited again. This hypothesis is consistent with another recent study in MDCK cells (Scheffers et al., 2004).

The findings of this study raise important questions about how migration of the cell sheet is initiated, how cues for migration are transmitted to cells that are distal to the edge and how collective cell migration is coordinated, allowing the sheet to move as a single unit despite the individual migratory behavior of the cells in the sheet. Answers to these questions will provide fundamental insight into epithelial cell-sheet migration that may help to illuminate strategies of collective cell migration in general and apply to in vivo tissue repair and embryonic development.

We thank Beat A. Imhof (Centre Medical Universitaire, Geneva, Switzerland) for the GFP-actin construct, and John D. Rafter and Wonhwa Cho (University of Illinois at Chicago) for help with two-photon microscopy. This work was supported by the National Institutes of Health (CA095177 to G.F.) and the American Cancer Society (RSG-02-250-01-DDC to G.F.).

References

Altan, Z. M. and Fenteany, G. (2004). c-Jun N-terminal kinase regulates lamellipodial protrusion and cell sheet migration during epithelial wound closure by a gene expression-independent mechanism. *Biochem. Biophys. Res. Commun.* **322**, 56-67.

Ballestrem, C., Wehrle-Haller, B. and Imhof, B. A. (1998). Actin dynamics in living mammalian cells. *J. Cell Sci.* **111**, 1649-1658.

Bement, W. M. (2002). Actomyosin rings: the riddle of the sphincter. *Curr. Biol.* **12**, R12-R14.

Bershadsky, A. D., Balaban, N. Q. and Geiger, B. (2003). Adhesion-dependent cell mechanosensitivity. *Annu. Rev. Cell Dev. Biol.* **19**, 677-695.

Block, E. R., Matela, A. R., SundarRaj, N., Iszkula, E. R. and Klarlund, J. K. (2004). Wounding induces motility in sheets of corneal epithelial cells through loss of spatial constraints: role of heparin-binding epidermal growth factor-like growth factor signaling. *J. Biol. Chem.* **279**, 24307-24312.

Buck, R. C. (1979). Cell migration in repair of mouse corneal epithelium. *Invest. Ophthalmol. Vis. Sci.* **18**, 767-784.

Burridge, K. and Wennerberg, K. (2004). Rho and Rac take center stage. *Cell* **116**, 167-179.

Carlier, M. F., Clainche, C. L., Wiesner, S. and Pantaloni, D. (2003). Actin-based motility: from molecules to movement. *Bioessays* **25**, 336-345.

Colas, J. F. and Schoenwolf, G. C. (2001). Towards a cellular and molecular understanding of neurulation. *Dev. Dyn.* **221**, 117-145.

Danjo, Y. and Gipson, I. K. (1998). Actin 'purse string' filaments are anchored by E-cadherin-mediated adherens junctions at the leading edge of the epithelial wound, providing coordinated cell movement. *J. Cell Sci.* **111**, 3323-3332.

Danjo, Y. and Gipson, I. K. (2002). Specific transduction of the leading edge cells of migrating epithelia demonstrates that they are replaced during healing. *Exp. Eye Res.* **74**, 199-204.

Davidson, L. A., Hoffstrom, B. G., Keller, R. and DeSimone, D. W. (2002). Mesendoderm extension and mantle closure in *Xenopus laevis* gastrulation: combined roles for integrin $\alpha_5\beta_1$, fibronectin, and tissue geometry. *Dev. Biol.* **242**, 109-129.

Desai, L. P., Aryal, A. M., Ceacareanu, B., Hassid, A. and Waters, C. M. (2004). RhoA and Rac1 are both required for efficient wound closure of airway epithelial cells. *Am. J. Physiol. Lung Cell Mol. Physiol.*

Dipasquale, A. (1975). Locomotion of epithelial cells. Factors involved in extension of the leading edge. *Exp. Cell Res.* **95**, 425-439.

Donaldson, D. J. and Dunlap, M. K. (1981). Epidermal cell migration during attempted closure of skin wounds in the adult newt: observations based on cytochalasin treatment and scanning electron microscopy. *J. Exp. Zool.* **217**, 33-43.

Fenteany, G. and Zhu, S. (2003). Small-molecule inhibitors of actin dynamics and cell motility. *Curr. Topics Med. Chem.* **3**, 593-616.

Fenteany, G., Janmey, P. A. and Stossel, T. P. (2000). Signaling pathways and cell mechanics involved in wound closure by epithelial cell sheets. *Curr. Biol.* **10**, 831-838.

Friedl, P. (2004). Prespecification and plasticity: shifting mechanisms of cell migration. *Curr. Opin. Cell Biol.* **16**, 14-23.

Friedl, P. and Wolf, K. (2003). Tumour-cell invasion and migration: diversity and escape mechanisms. *Nat. Rev. Cancer* **3**, 362-374.

Friedl, P., Hegerfeldt, Y. and Tusch, M. (2004). Collective cell migration in morphogenesis and cancer. *Int. J. Dev. Biol.* **48**, 441-449.

Garlick, J. A. and Taichman, L. B. (1994). Fate of human keratinocytes during re-epithelialization in an organotypic culture model. *Lab. Invest.* **70**, 916-924.
Gibbins, J. R. (1978). Epithelial migration in organ culture. A morphological and time lapse cinematographic analysis of migrating stratified squamous epithelium. *Pathology* **10**, 207-218.
Goldmann, W. H. (2002). Mechanical aspects of cell shape regulation and signaling. *Cell Biol. Int.* **26**, 313-317.
Hanna, C. (1966). Proliferation and migration of epithelial cells during corneal wound repair in the rabbit and the rat. *Am. J. Ophthalmol.* **61**, 55-63.
Harden, N. (2002). Signaling pathways directing the movement and fusion of epithelial sheets: lessons from dorsal closure in *Drosophila*. *Differentiation* **70**, 181-203.
Hinman, L. E., Beilman, G. J., Groehler, K. E. and Sammak, P. J. (1997). Wound-induced calcium waves in alveolar type II cells. *Am. J. Physiol.* **273**, L1242-1248.
Howat, W. J., Holgate, S. T. and Lackie, P. M. (2002). TGF-β isoform release and activation during *in vitro* bronchial epithelial wound repair. *Am. J. Physiol. Lung Cell Mol. Physiol.* **282**, L115-L123.
Ikenoya, M., Hidaka, H., Hosoya, T., Suzuki, M., Yamamoto, N. and Sasaki, Y. (2002). Inhibition of Rho-kinase-induced myristoylated alanine-rich C kinase substrate (MARCKS) phosphorylation in human neuronal cells by H-1152, a novel and specific Rho-kinase inhibitor. *J. Neurochem.* **81**, 9-16.
Ingber, D. E. (2003). Mechanobiology and diseases of mechanotransduction. *Ann. Med.* **35**, 564-577.
Isakson, B. E., Evans, W. H. and Boitano, S. (2001). Intercellular Ca^{2+} signaling in alveolar epithelial cells through gap junctions and by extracellular ATP. *Am. J. Physiol. Lung Cell Mol. Physiol.* **280**, L221-228.
Jacinto, A., Martinez-Arias, A. and Martin, P. (2001). Mechanisms of epithelial fusion and repair. *Nat. Cell Biol.* **3**, E117-E123.
Jacinto, A., Woolner, S. and Martin, P. (2002). Dynamic analysis of dorsal closure in *Drosophila*: from genetics to cell biology. *Dev. Cell* **3**, 9-19.
Janmey, P. A. and Weitz, D. A. (2004). Dealing with mechanics: mechanisms of force transduction in cells. *Trends Biochem. Sci.* **29**, 364-370.
Kartha, S. and Toback, F. G. (1992). Adenine nucleotides stimulate migration in wounded cultures of kidney epithelial cells. *J. Clin. Invest.* **90**, 288-292.
Keller, R. (2002). Shaping the vertebrate body plan by polarized embryonic cell movements. *Science* **298**, 1950-1954.
Keller, R., Davidson, L. A. and Shook, D. R. (2003). How we are shaped: the biomechanics of gastrulation. *Differentiation* **71**, 171-205.
Kiehart, D. P. (1999). Wound healing: the power of the purse string. *Curr. Biol.* **9**, R602-R605.
Klepeis, V. E., Cornell-Bell, A. and Trinkaus-Randall, V. (2001). Growth factors but not gap junctions play a role in injury-induced Ca^{2+} waves in epithelial cells. *J. Cell Sci.* **114**, 4185-4195.
Kolega, J. (1981). The movement of cell clusters *in vitro*: morphology and directionality. *J. Cell Sci.* **49**, 15-32.
Kolega, J. (1986). Effects of mechanical tension on protrusive activity and microfilament and intermediate filament organization in an epidermal epithelium moving in culture. *J. Cell Biol.* **102**, 1400-1411.
Krawczyk, W. S. (1971). A pattern of epidermal cell migration during wound healing. *J. Cell Biol.* **49**, 247-263.
Lee, T. Y. and Gotlieb, A. I. (2003). Microfilaments and microtubules maintain endothelial integrity. *Microsc. Res. Tech.* **60**, 115-127.
Lubarsky, B. and Krasnow, M. A. (2003). Tube morphogenesis: making and shaping biological tubes. *Cell* **112**, 19-28.
Mahan, J. T. and Donaldson, D. J. (1986). Events in the movement of newt epidermal cells across implanted substrates. *J. Exp. Zool.* **237**, 35-44.
Martin, P. and Parkhurst, S. M. (2004). Parallels between tissue repair and embryo morphogenesis. *Development* **131**, 3021-3034.
McHenry, K. T., Ankala, S. V., Ghosh, A. K. and Fenteany, G. (2002). A non-antibacterial oxazolidinone derivative that inhibits epithelial cell sheet migration. *Chembiochem* **11**, 1105-1111.
Nelson, W. J. (2003). Tube morphogenesis: closure, but many openings remain. *Trends Cell Biol.* **13**, 615-621.
Nuccitelli, R. (2003). A role for endogenous electric fields in wound healing. *Curr. Top. Dev. Biol.* **58**, 1-26.
Omelchenko, T., Vasiliev, J. M., Gelfand, I. M., Feder, H. H. and Bonder, E. M. (2003). Rho-dependent formation of epithelial "leader" cells during wound healing. *Proc. Natl. Acad. Sci. USA* **100**, 10788-10793.
Pollard, T. D. and Borisy, G. G. (2003). Cellular motility driven by assembly and disassembly of actin filaments. *Cell* **112**, 453-465.
Quilhac, A. and Sire, J. Y. (1999). Spreading, proliferation, and differentiation of the epidermis after wounding a cichlid fish, *Hemichromis bimaculatus*. *Anat. Rec.* **254**, 435-451.
Radice, G. P. (1980a). Locomotion and cell-substratum contacts of *Xenopus* epidermal cells *in vitro* and *in situ*. *J. Cell Sci.* **44**, 201-223.
Radice, G. P. (1980b). The spreading of epithelial cells during wound closure in *Xenopus* larvae. *Dev. Biol.* **76**, 26-46.
Rafelski, S. M. and Theriot, J. A. (2004). Crawling toward a unified model of cell motility: spatial and temporal regulation of actin dynamics. *Annu. Rev. Biochem.* **73**, 209-239.
Raftopoulou, M. and Hall, A. (2004). Cell migration: Rho GTPases lead the way. *Dev. Biol.* **265**, 23-32.
Rand, H. W. (1915). Wound closure in actinian tentacles with reference to the problem of organization. *Rouxs Arch. Entwicklungsmech. Organismen* **41**, 159-214.
Redd, M. J., Cooper, L., Wood, W., Stramer, B. and Martin, P. (2004). Wound healing and inflammation: embryos reveal the way to perfect repair. *Philos. Trans. R. Soc. Lond., B, Biol. Sci.* **359**, 777-784.
Revenu, C., Athman, R., Robine, S. and Louvard, D. (2004). The co-workers of actin filaments: from cell structures to signals. *Nat. Rev. Mol. Cell Biol.* **5**, 635-646.
Ridley, A. J., Schwartz, M. A., Burridge, K., Firtel, R. A., Ginsberg, M. H., Borisy, G., Parsons, J. T. and Horwitz, A. R. (2003). Cell migration: integrating signals from front to back. *Science* **302**, 1704-1709.
Rosen, P. and Misfeldt, D. S. (1980). Cell density determines epithelial migration in culture. *Proc. Natl. Acad. Sci. USA* **77**, 4760-4763.
Saitoh, M., Ishikawa, T., Matsushima, S., Naka, M. and Hidaka, H. (1987). Selective inhibition of catalytic activity of smooth muscle myosin light chain kinase. *J. Biol. Chem.* **262**, 7796-7801.
Scheffers, M. S., van der Bent, P., van de Wal, A., van Eendenburg, J., Breuning, M. H., de Heer, E. and Peters, D. J. (2004). Altered distribution and co-localization of polycystin-2 with polycystin-1 in MDCK cells after wounding stress. *Exp. Cell Res.* **292**, 219-230.
Simske, J. S. and Hardin, J. (2001). Getting into shape: epidermal morphogenesis in *Caenorhabditis elegans* embryos. *Bioessays* **23**, 12-23.
Small, J. V., Stradel, T., Vignal, E. and Rottner, K. (2002). The lamellipodium: where motility begins. *Trends Cell Biol.* **12**, 112-120.
Sponsel, H. T., Breckon, R., Hammond, W. and Anderson, R. J. (1994). Mechanisms of recovery from mechanical injury of renal tubular epithelial cells. *Am. J. Physiol.* **267**, F257-F264.
Sponsel, H. T., Breckon, R. and Anderson, R. J. (1995). Adenine nucleotide and protein kinase C regulation of renal tubular epithelial cell wound healing. *Kidney Int.* **48**, 85-92.
Stahelin, R. V., Digman, M. A., Medkova, M., Ananthanarayanan, B., Rafter, J. D., Melowic, H. R. and Cho, W. (2004). Mechanism of diacylglycerol-induced membrane targeting and activation of protein kinase Cδ. *J. Biol. Chem.* **279**, 29501-29512.
Straight, A. F., Cheung, A., Limouze, J., Chen, I., Westwood, N. J., Sellers, J. R. and Mitchison, T. J. (2003). Dissecting temporal and spatial control of cytokinesis with a myosin II Inhibitor. *Science* **299**, 1743-1747.
Strohmeier, R. and Bereiter-Hahn, J. (1991). Emigration of bilayered epidermal cell sheets from tadpole tails (*Xenopus laevis*). *Cell Tissue Res.* **266**, 615-621.
Trinkaus, J. P. (1984). *Cells into Organs: The Forces that Shape the Embryo.* Englewood Cliffs, NJ: Prentice Hall.
Uehata, M., Ishizaki, T., Satoh, H., Ono, T., Kawahara, T., Morishita, T., Tamakawa, H., Yamagami, K., Inui, J., Maekawa, M. et al. (1997). Calcium sensitization of smooth muscle mediated by a Rho-associated protein kinase in hypertension. *Nature* **389**, 990-994.
Vaughan, R. B. and Trinkaus, J. P. (1966). Movements of epithelial cell sheets *in vitro*. *J. Cell Sci.* **1**, 407-413.
Welch, M. D. and Mullins, R. D. (2002). Cellular control of actin nucleation. *Annu. Rev. Cell Dev. Biol.* **18**, 247-288.
Woolley, K. and Martin, P. (2000). Conserved mechanisms of repair: from damaged single cells to wounds in multicellular tissues. *Bioessays* **22**, 911-919.
Zhao, M., Song, B., Pu, J., Forrester, J. V. and McCaig, C. D. (2003). Direct visualization of a stratified epithelium reveals that wounds heal by unified sliding of cell sheets. *FASEB J.* **17**, 397-406.

Journal of Cell Science